NEOPLASIA
www.neoplasia.com

Volume 20 Number 10 October 2018 pp. 985–995 985

DDK Has a Primary Role in Processing Stalled Replication Forks to Initiate Downstream Checkpoint Signaling

Nanda Kumar Sasi[*,†,‡], Flavie Coquel[§], Yea-Lih Lin[§], Jeffrey P MacKeigan[†], Philippe Pasero[§] and Michael Weinreich[*]

[*]Laboratory of Genome Integrity and Tumorigenesis, Van Andel Research Institute (VARI), Grand Rapids, MI 49503; [†]Laboratory of Systems Biology, VARI; [‡]Graduate Program in Genetics, Michigan State University, East Lansing, MI 48824; [§]IGH, Institute of Human Genetics CNRS UMR 9002 and University of Montpellier, Equipe Labellisée Ligue contre le Cancer, 141 rue de la Cardonille 34396 Cedex 5, Montpellier, France

Summary

CDC7-DBF4 kinase (DDK) initiates DNA replication in eukaryotes by activating the replicative MCM helicase. DDK has diverse and apparently conflicting roles in the replication checkpoint response in various organisms, but the underlying mechanisms are far from settled. We show that human DDK promotes limited resection of newly synthesized DNA at stalled replication forks or sites of DNA damage to initiate replication checkpoint signaling. DDK is also required for efficient fork restart and G2/M cell cycle arrest. DDK exhibits genetic interactions with the ssDNA exonuclease EXO1 and phosphorylates EXO1 *in vitro*. EXO1 is also required for nascent strand degradation following exposure to HU, so DDK might regulate EXO1 directly. Lastly, sublethal DDK inhibition causes various mitotic abnormalities, which is consistent with a checkpoint deficiency. In summary, DDK has a primary and previously undescribed role in the replication checkpoint to promote ssDNA accumulation at stalled forks, which is required to initiate a robust checkpoint response and cell cycle arrest to maintain genome integrity.

Neoplasia (2018) 20, 985–995

Introduction

DDK is a two-subunit kinase that is essential to initiate DNA replication at individual replication origins by phosphorylating and activating the MCM2-7 replicative helicase. The regulatory subunit DBF4 binds to CDC7 and is required for its kinase activity [1]. DDK also has roles in replication checkpoint signaling that are less well understood [1]. In budding yeast, DDK is a target of the checkpoint effector kinase Rad53 that is activated following replication stress [2]. Rad53-mediated phosphorylation of Dbf4 modestly reduces DDK activity [2] and also inhibits late origin firing [3], but there is also evidence that DDK is required for the complete activation of Rad53 kinase [4]. In fission yeast, DDK subunits Hsk1 and Dfp1 are phosphorylated upon HU treatment by the checkpoint kinase Cds1, orthologous to budding yeast Rad53 and mammalian CHK2 [5]. Deletion of Cds1 partially rescues the temperature sensitivity of *hsk1-1312* mutants, suggesting that Cds1 (like Rad53) inhibits DDK activity [5]. Cds1 activation in response to HU, however, was reduced significantly in *hsk1*(ts) strains at restrictive temperature, and the cell cycle arrest was also aberrant as seen by an increased population of "cut" cells (indicative of mitosis without complete DNA replication) [5,6]. These paradoxical results in yeast could be explained by a negative feedback loop where DDK first helps to initiate replication checkpoint activation and then the checkpoint pathway subsequently alters DDK activity to inhibit late origin firing.

Initial studies in human cells showed that the replication checkpoint inhibits DDK activity, presumably to inhibit origin firing [7]. However, subsequent studies reported that human DDK is active during replication stress and has an upstream role to fully activate the checkpoint kinase CHK1 [8,9]. In response to exogenous replication inhibitors, DDK

Abbreviations: DDK, CDC7-DBF4 kinase; HU, Hydroxyurea; CPT, Camptothecin

Address all correspondence to: Michael Weinreich, PhD, Van Andel Research Institute, 333 Bostwick Ave. NE, Grand Rapids, MI 49503, USA.
E-mail: michael1@mit.edu

Received 20 April 2018; Revised 1 August 2018; Accepted 2 August 2018

1476-5586
https://doi.org/10.1016/j.neo.2018.08.001

recruitment to chromatin is increased [8,9], CDC7-DBF4 complex is stabilized [8], and MCM shows increased phosphorylation at several DDK-specific sites [8]. DDK promotes CHK1 phosphorylation partly through binding to and phosphorylating Claspin, an adaptor protein required for CHK1 activation [10,11]. Although depleting the CDC7 protein subunit using a CDC7 siRNA resulted in loss of chromatin-bound Claspin following HU treatment [10], inhibiting DDK activity using small molecule inhibitors did not [11]. Furthermore, depleting Claspin using siRNA did not reduce CHK1 phosphorylation to the same extent as CDC7 siRNA [10], suggesting that DDK could promote checkpoint signaling by other mechanisms.

In this study, we show that DDK has a novel and primary role to initiate checkpoint signaling by promoting ssDNA formation at stalled forks, most likely by promoting nascent DNA resection. DDK activity is also required for efficient restart of damaged replication forks. Lastly, low-dose DDK inhibition results in cells that progress through mitosis with anaphase bridges and other aberrant structures indicative of problems in completing DNA replication and in maintaining a stable G2/M arrest. Based on these findings, we propose a model explaining the role of DDK in activating checkpoint signaling and maintaining genome integrity.

Material and Methods

Cell Lines and Reagents

HCC1954 cells (ATCC) and Colo-205 (NCI-60) were cultured in RPMI-1640 media supplemented with 10% heat inactivated (HI) FBS, 50 U/ml of penicillin, and 50 μg/ml of streptomycin. HEK-293FT packaging cells for generating lentiviral particles were maintained in DMEM supplemented with 10% BCS, 50 U/ml of penicillin, and 50 μg/ml of streptomycin. hEXO1 cDNA with C-terminal MYC tag was inserted into pCW57-MCS1-P2A-MCS2 (Addgene plasmid # 80921, gift from Adam Karpf) by GIBSON assembly. HCC1954 cells stably expressing Dox-inducible EXO1b-MYC were created by lentiviral infection followed by selection in 5 μg/ml blasticidin. Protein expression was induced with 2 μg/ml Doxycylin.

The DDK inhibitors, PHA-767491 and XL413, were synthesized as described previously [12]. ATR inhibitor (VE-821, #A2521) and Camptothecin (#A2877) were from APExBIO. CHK1 inhibitor (LY2603618, #S2626) was from Selleckchem. Etoposide (#341205) was from EMD Millipore. Hydroxyurea (#H9120) was from USBiological. The antibodies were purchased as indicated: CST: PARP (#9542), pCHK1 S317 (#12302), pCHK1 S345 (#2348), pCHK1 S296 (#2349), CHK1 (#2360), pCHK2 T68 (#2197), CHK2 (#6334), RAD51 (#8875), CtIP (#93110); Bethyl Laboratories Inc.: pMCM2 S53 (A300-756A), MCM2 (A300-122A), pRPA2 S33 (A300-246A), pRPA2 S4/S8 (A300-245A), ORC2 (A302–735A), EXO1 (A302-639A), MRE11 (A303-998A), BLM (A300-110A); MBL International Corporation: CDC7 (K0070-3S); Sigma: β-actin (A5441), Tubulin (T9026); antibodies against RPA1 (NA13, EMD Millipore) and RPA2 (04–1481, EMD Millipore) were gifts from Dr. Bruce Stillman; GE Healthcare: anti-mouse-HRP (NA931V), and anti-rabbit-HRP (NA934V).

RNAi Interference

HCC1954 cells were plated in 6-well plates (75,000 cells/well) allowed to grow for 36 hours before transfection. siRNA transfection was performed with Lipofectamine RNAiMAX (Invitrogen) according to manufacturer's instructions. Each well was transfected with 2 μl transfection reagent and a final siRNA concentration of 25 nM (*CDC7*, *EXO1*) or 5 nM (*MRE11*, *CtIP*, *BLM*) in a total volume of 2 ml. Medium was replaced 24 hours after transfection, and the cells were either harvested or exposed to indicated treatments 48 hours after transfection. Following siRNAs were used: *CDC7* (CDC7-L1, Dharmacon custom siRNA, GGCAAGATAATGTCATGGGA), *EXO1 #1* (Qiagen, SI02665145), *EXO1 #2 (*Qiagen, SI00054705), *EXO1 #3 (*Qiagen, SI02665138), *MRE11A* (Thermo Scientific, #s8960), *CtIP* (Thermo Scientific, #s142451), *BLM* (Thermo Scientific #s1999).

Immunoblotting and Protein Fractionation

Whole cell extracts were prepared by resuspending the pellets in RIPA buffer (150 mM NaCl, 1% NP-40, 0.5% sodium deoxycholate, 0.1% SDS, 50 mM Tris-HCl, pH 8) containing protease inhibitors (100 μM PMSF, 1 mM Benzamidine, 2.5 μg/ml Pepstatin A, 10 μg/ml Leupeptin, and 10 μg/ml Aprotinin) and phosphatase inhibitors (1 mM each NaF, Na_3VO_4, $Na_2P_2O_7$). Protein concentration was measured using the BCA protein assay kit (Pierce, #23227). Cell fractionation into cytosolic, nuclear-soluble, and nuclear-insoluble (chromatin) fractions was performed as described previously [13]. Pellets were resuspended in lysis Buffer A (10 mM HEPES (pH 7.9), 10 mM KCl, 1.5 mM $MgCl_2$, 0.34 M Sucrose, 10% Glycerol, 1 mM DTT, and protease and phosphatase inhibitors), and Triton X-100 was added to a final concentration of 0.1%. After incubation on ice for 8 minutes, lysates were centrifuged at 1300*g*, at 4°C, for 5 minutes. The supernatant was collected and clarified by high-speed centrifugation (20,000*g*, 4°C, 5 minutes) to obtain cytosolic fraction. The pellet was washed once with Buffer A and then lysed in Buffer B (3 mM EDTA, 0.2 mM EGTA, 1 mM DTT, protease and phosphatase inhibitors) for 30 minutes on ice. Soluble nuclear fraction (supernatant) was collected by centrifugation at 1700*g*, at 4°C, for 5 minutes. The chromatin fraction (pellet) was washed once with Buffer B, resuspended in Buffer B, and sonicated briefly. Protein concentration in each fraction was measured using Bradford assay (Bio Rad, #500-0006). Equal amounts of proteins were subjected to SDS-PAGE and transferred to nitrocellulose membrane (Millipore, HATF304F0). Transfer efficiency and equal loading were confirmed by Ponceau S staining. Membranes were blocked overnight at 4°C with 5% nonfat milk in TBS-T followed by incubation in primary and secondary antibodies (1 hour at RT, 2% milk in TBS-T). Protein bands were visualized using SuperSignal West Pico solutions (Thermo Scientific).

Analysis of Caspase 3/7 Activity

A total of 5000 cells per well were plated in 96-well plates. Twenty-four hours later, cells were treated and incubated for the indicated period of time at 37°C. Caspase 3/7 activity and viable cell number were then measured using the Caspase-Glo 3/7 assay (Promega) and CellTiter-Glo assay (Promega), respectively. The "caspase activity per cell" was obtained by normalizing total caspase activity to cell number. Luminescence was measured using BioTek Synergy Microplate Reader 30 minutes after addition of 'Glo' reagents.

Cell Cycle Analysis

Cells were trypsinized, washed twice with cold PBS, and fixed/permeabilized in 70% ice-cold ethanol (made in water). After fixation on ice for 30 minutes, cells were centrifuged at 400*g* (4°C, for 5

minutes), washed once with cold PBS, and centrifuged again. The pellets were resuspended in analysis buffer (10 μg/ml propidium iodide and 250 μg/ml RNAase) and incubated at 37°C for 30 minutes. Cell cycle profiles were obtained using FACSCalibur (BD Biosciences) flow cytometer. The data were analyzed using Flowing Software.

Immunofluorescence

HCC1954 cells were seeded at 50,000 to 70,000 cells per well on number 1.5 coverglass in 24-well tissue culture dishes. siRNA-mediated knockdown was carried out in six-well plates. Twenty-four hours later, the cells were trypsinized and replated on coverglass in 24-well plates. After 36 hours, cells were treated as indicated. For RPA2 and BrdU immunofluorescence analysis, cells were washed with 1× PBS, preextracted with 0.2% Triton X-100 (in PBS) for 5 minutes, washed twice with 1× PBS, and fixed in 4% paraformaldehyde for 10 minutes at room temperature. Cells were then stained with primary antibody (1:1000 in DMEM + 10% FBS + 0.01% sodium azide) overnight at 4°C on a shaker. After three 5-minute washes with PBS-T (0.01% Tween 20), cells were incubated in Alexa Fluor 488 secondary antibody (#A-11001, 1:1000 in DMEM + 10% FBS + 0.01% sodium azide) for 1 hour followed by three washes with PBS-T. Nuclear DNA was stained with Hoechst 33342 (2 μg/ml). Coverglass was inverted onto microscope slides using mounting gel. Cells were imaged using a 60× oil-immersion objective on a Nikon Eclipse Ti florescent microscope. Image processing and quantification were completed with NIS Elements software (Nikon). To quantify, regions of interest (ROIs) were drawn around each nucleus. Using HU-treated cells as a positive control, intensity thresholds (binary) were set to include all pixels equal to or greater than the intensity of the background 488 fluorescence. The binary was applied to all samples, and the sum intensity of the "binary in ROI" was calculated for each nucleus. All values were normalized to the mean intensity of the vehicle control. For analysis of mitotic abnormalities, cells were fixed and permeabilized in 70% ethanol. Nuclear DNAthyc=5?> was stained with Hoechst 33342 (2 μg/ml). Image analysis was performed using NIS Elements software (Nikon). Statistical analysis was performed using Graph Pad Prism.

DNA Fiber Spreading

DNA fiber spreading was performed as described previously [14,15]. Briefly, subconfluent cells were sequentially labeled first with 10 μM 5-iodo-2′-deoxyuridine (IdU) and then with 100 μM 5-chloro-2′-deoxyuridine (CldU) for the indicated times. One thousand cells were loaded onto a glass slide (Star Frost) and lysed with spreading buffer (200 mM Tris-HCl pH 7.5, 50 mM EDTA, 0.5% SDS) by gently stirring with a pipette tip. The slides were tilted slightly, and the surface tension of the drops was disrupted with a pipette tip. The drops were allowed to run down the slides slowly, then air-dried, fixed in methanol/acetic acid 3:1 for 10 minutes, and allowed to dry. Glass slides were processed for immunostaining with mouse anti-BrdU to detect IdU (347,580, BD Biosciences), rat anti-BrdU (ABC117–7513, Eurobio Abcys) to detect CldU, mouse anti-ssDNA (MAB3868, Millipore) antibodies, and corresponding secondary antibodies conjugated to various Alexa Fluor dyes. Nascent DNA fibers were visualized by using immunofluorescence microscopy (Zeiss Apotome 2). The acquired DNA fiber images were analyzed by using MetaMorph Microscopy Automation and Image Analysis Software (Molecular Devices), and statistical analysis was performed with Graph Pad Prism (Graph Pad Software). The lengths of at least 150 IdU/CldU tracks were measured per sample.

Protein Purification

Human DDK was purified as described previously [12]. Recombinant human EXO1 protein was produced in *Escherichia coli* BL21-CodonPlus-(DE3)-RIL cells (Agilent Technologies) with the construct pTXB1-hExo1 WT (gift from S. Ferrari to Titia de Lange) as described previously [16]. Expression of EXO1 was induced with 0.2 mM IPTG at 18°C for 12 hours. The bacterial pellet was washed with cold PBS, resuspended in lysis buffer (50 mM Tris-HCl 8, 500 mM NaCl, 1 mM EDTA, 10% glycerol, 0.1% Triton X-100, with protease inhibitors), and sonicated. The supernatant was purified using chitin beads (NEB #S6651S) according to manufacturer's instructions. The eluate was further purified on a 5-ml HighTrap SP column (Amersham Pharmacia, Uppsala, Sweden) equilibrated with a buffer containing 50 mM Tris-HCl pH 7.5, 0.1 mM EDTA, 10% glycerol, 1 mM DTT, and 150 mM NaCl. Proteins were eluted with a linear concentration gradient of NaCl (0-1 M) and stored at −80°C.

In Vitro Kinase Assay

Approximately 115 ng of purified full length EXO1 or 100 ng of BSA was incubated with 20 ng of purified human DDK in a reaction mixture containing 10 μCi (γ)-^{32}P ATP, 100 μM cold ATP, 50 mM Tris-HCl (pH 7.5), 10 mM $MgCl_2$, and 1 mM DTT and incubated for 30 minutes at 30°C. The proteins were denatured in 1× Laemmli buffer at 100°C followed by SDS-PAGE and autoradiography on Phosphoimager (Fuji). Identical samples without (γ)-^{32}P ATP were used for Coomasie staining and immunoblot analysis.

Results and Discussion

DDK Has a Primary Role in Initiating Replication Checkpoint Signaling

Since blocking DDK activity largely prevents CHK1 phosphorylation upon exposure to replication stress [9–11], we analyzed how DDK influences the overall checkpoint response induced by HU. We found that 5 μM of DDKi and a pretreatment time of 4 hours substantially blocked CHK1 activation by HU in HCC1954 cells (Supplementary Figure 1*A*). HCC1954 is a breast cancer cell line that expresses high levels of both DDK subunits and exhibits robust decrease in MCM2 phosphorylation in response to the prototype DDK inhibitor PHA-767491 (hereafter referred to as DDKi) [12]. CHK1 activation following HU addition was almost completely eliminated by the DDKi (Figure 1*A*) and as shown previously [11]. A similar effect on CHK1 activation was seen in response to the more specific DDK inhibitor XL413 in Colo-205 cells (Figure 1*B*). However, unexpectedly, we found that RPA2 S4/S8 phosphorylation and RPA chromatin accumulation following HU exposure were also significantly reduced if DDK activity was blocked (Figure 1*A*, *B*). Since these events are upstream of Chk1 activation, this result was not consistent with a singular role for DDK to promote CHK1 activation through Claspin phosphorylation. We saw an identical decrease in RPA2 S4/S8 phosphorylation and chromatin accumulation when DDK activity was blocked using an siRNA against *CDC7* (Supplementary Figure 1*B*). Chromatin-bound RPA2 immunofluorescence, which is sharply increased after 2 hours of HU exposure, was also significantly reduced in CDC7 siRNA-treated cells (Supplementary Figure 1*C*). DDK inhibition also prevented CHK1 phosphorylation, RPA2 accumulation,

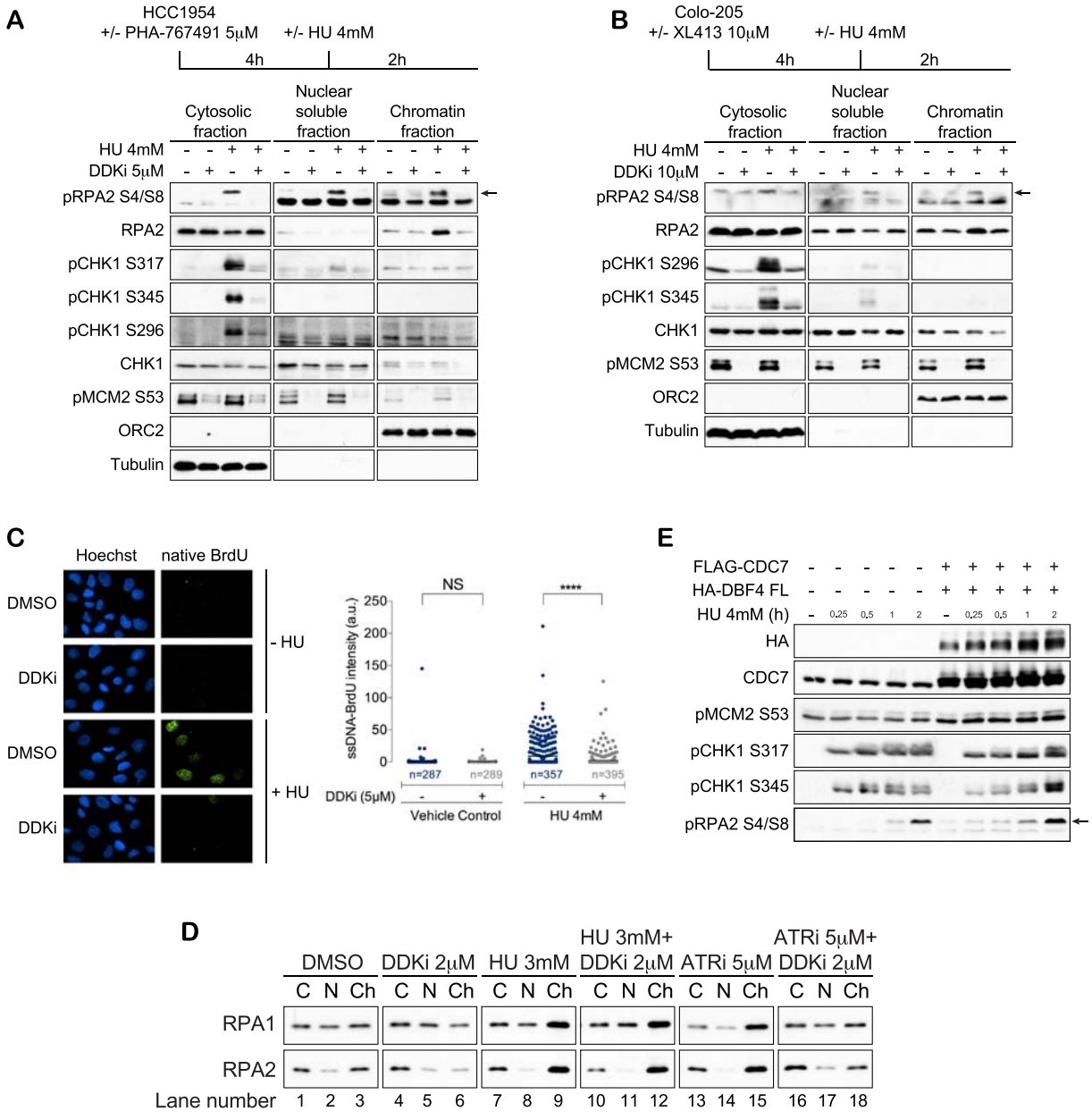

Figure 1. DDK activity is required for generating ssDNA and initiating the checkpoint pathway. (A) HCC1954 cells or (B) Colo-205 cells were pretreated with DMSO or DDKi for 4 hours followed by incubation with or without HU for 2 hours, cell fractionation, and immunoblot analysis. Arrow indicates RPA phosphorylated at S4/S8. (C) BrdU-treated HCC1954 cells were treated as in (A) and analyzed using immunofluorescence microscopy. (D) HCC1954 cells were treated with indicated drugs for 2 hours followed by cell fractionation and immunoblot analysis. *C*, cytoplasmic; *N*, nuclear soluble; *Ch*, chromatin fraction. (E) HEK-293 T cells were transfected with indicated constructs and, 48 hours later, treated with HU for the indicated time.

and RPA2 S4/S8 phosphorylation in response to two DNA damaging agents, camptothecin and etoposide (Supplementary Figure 1*D*, *E*). Using a nondenaturing BrdU assay that directly measures ssDNA formation, we found that the ssDNA formation upon HU treatment was significantly reduced upon DDK inhibition (Figure 1*C*). DDK inhibition alone, in the absence of exogenous replication inhibitors, did not result in widespread ssDNA formation or the activation of replication-checkpoint signaling (Supplementary Figure 2*A*, *B*), confirming several earlier findings [17,18]. RPA2-S33 was only mildly phosphorylated in response to the DDK inhibitor, which is also not consistent with robust checkpoint activation since RPA2-S33 is hyperphosphorylated upon replication stress [19]. Taken together, our results show that DDK inhibition substantially blocks the accumulation of ssDNA and downstream events (i.e., RPA binding to ssDNA) in response to replication fork stalling by HU or DNA damage by camptothecin and etoposide.

While reduced origin firing upon DDK inhibition might explain the lack of checkpoint activation in response to HU, several pieces of evidence argue against this and suggest a more direct role for DDK at stalled forks. First, we took advantage of the fact that inhibiting ATR kinase in unperturbed cells induces aberrant origin firing leading to accumulation of chromatin-bound RPA1 and RPA2 (Figure 1*D*, **lane 3 vs. 15**), as previously shown [20]. This RPA accumulation at new

origins, however, was prevented upon co-treatment with DDKi (Figure 1*D*, **lane 15 vs. 18**) consistent with the essential role of DDK in origin firing. In contrast, HU-mediated RPA accumulation on chromatin, which is blocked by prior treatment with DDKi, was not affected by co-treatment with DDKi (Figure 1*D*, **lane 9 vs. 12**). This argues that the RPA accumulation seen in HU is predominantly occuring at stalled forks and DDKi prevents this accumulation. We also found that overexpressing human DDK subunits increased the phosphorylation of CHK1 and RPA2 in response to HU treatment (Figure 1*E*), again consistent with a positive role for DDK in promoting checkpoint activation.

Several studies in yeast also suggest that DDK plays a direct role in the replication checkpoint. In fission yeast, the *hsk1-89* temperature-sensitive strain that alters the Cdc7 subunit showed ~20-fold reduction in Cds1 (Rad53/CHK2) activation following HU treatment, even at permissive temperature [6]. However, other fission yeast mutants defective in origin firing (e.g., *mcm4* or *orc1* mutants) did not show a similar reduction in Cds1 activation [6], suggesting an origin-independent role for Hsk1 (CDC7) in Cds1 activation. Budding yeast *cdc7* and *dbf4* mutants also have substantially reduced levels of Rad53 [21]. In summary, our results indicate that DDK promotes formation of ssDNA-RPA complexes upon exposure to various forms of replication stress independently of its role in origin activation. This was confirmed below using single molecule analyses to restrict the analysis of DDK to sites of ongoing DNA replication.

DDK Is Required for Processing Stalled Replication Forks

Based on the findings described above, we hypothesized that DDK is required to process stalled replication forks to activate the replication checkpoint in human cells. To test this directly, we performed DNA fiber analysis and measured the effect of inhibiting DDK on newly formed DNA strands at established forks (Figure 2*A*). Cells pretreated with or without DDKi were exposed to short (20 minutes) consecutive pulses of IdU and CldU followed by treatment with or without HU for 2 hours. A shorter incorporation time allowed detection of smaller changes in the length of nascent DNA (measured as CldU track length) than in previously published assays (P. Pasero, unpublished data). Treatment with DDKi alone had little effect on CldU track length, indicating that DDK inhibition does not alter nascent strand length in unperturbed cells (Figure 2*B* and *C*, **DMSO vs. DDKi 2 h, DDKi 4 h**). Moreover, DDKi-treated samples did not show an appreciable decrease in the density of replication fibers (not shown), indicating that sufficient replication forks exist in these cells to activate a checkpoint response. We found that 2 hours of HU exposure significantly reduced the length of nascent DNA tracks (CldU tracks) in HCC1954 cells compared to untreated cells (Figure 2*B*, **DMSO vs. DMSO + HU**). A reduction in the ratio of CldU to IdU lengths was also observed upon 2 hours of HU treatment, which normalizes for any change in the rates of replication elongation (Figure 2*C*, **DMSO vs. DMSO + HU**). Similar shortening of nascent DNA tracts was observed in HU-treated MCF-7 cells (Supplementary Figure 3*A-C*) and in several different cell lines irrespective of their genetic backgrounds, with tract-length shortening directly correlated with the time of incubation in HU (P. Pasero, unpublished data).

Importantly, DDKi treatment prevented degradation of nascent DNA upon HU exposure (Figure 2*B*, and *C*, **DMSO + HU vs. DDKi 2 h/4 h + HU**). The reduction in nascent strand degradation was correlated with the extent of DDK inhibition, with 4 hours of DDKi pretreatment resulting in CldU track lengths similar to DMSO treated cells (Figure 2*B*). We find that RPA accumulation on chromatin correlates well with the length of nascent DNA seen in DNA fiber assay (Figures 1*A*, *B* and 2*B*, *C*). Based on these data, we propose that DDK actively promotes limited resection of stalled replication forks, which is required for formation of ssDNA, local accumulation of RPA, and activation of downstream checkpoint signaling.

In a Xenopus *in vitro* system, aphidicolin treatment, which inhibits DNA polymerase alpha and delta, results in unrestricted DNA unwinding and ssDNA formation ahead of the stalled fork that is thought to induce the replication checkpoint [22]. This was proposed to be due to a functional (but not physical) uncoupling of the replicative polymerases and helicase (see model in Figure 4*F*). Given that helicase and polymerase activities are strongly interdependent and depend on physical interactions in many model organisms [23–25], it is not clear how a functional uncoupling might result in independent helicase activity in living cells. Electron microscopic analysis has shown that ssDNA formed in yeast at stalled forks is limited to one parental strand [26]. However, uncoupling between the polymerase and helicase would generate long ssDNA on both leading and lagging strands. In addition, diverse types of replication inhibitors generate ssDNA, even interstrand crosslinking agents, which would not allow helicase activity or polymerase activity beyond the crosslink. So, while helicase-polymerase uncoupling can generate ssDNA ahead of the forks in response to certain types of replication stress, our data suggest that DDK-dependent limited processing of nascent DNA behind stalled forks might be a commonly used mechanism for ssDNA formation behind forks.

DDK Is Required for Restart of Stalled Replication Forks

An important function of the replication checkpoint pathway is to promote DNA repair mechanisms required for rescuing and restarting stalled forks [1]. Using a DNA fiber assay, we measured the rate of fork restart following 1 or 2 hours of CPT exposure (Figure 2*C*) since CPT treatment damages DNA and replication restart depends on successful DNA repair. If DDK is required for fork restart, we would expect to see a reduced rate of fork restart in CPT + DDKi–treated cells compared to CPT treatment alone. Sixty-four percent of forks restarted after 1 hour of 1 μM CPT exposure, and this was reduced to 46% when cells were pretreated with DDKi for 4 hours (Figure 2*D*). The effect of 2 hours of CPT on fork restart was more severe with only 40% of forks restarting after removal of CPT. This was further reduced to 27% when they were pretreated with DDKi for 4 hours (Figure 2*E*). These results confirm that DDK is required for efficient replication fork restart, presumably because cells are defective in initiating the replication checkpoint and DNA repair and therefore cannot efficiently restart stalled replication forks.

DDK Might Regulate Nuclease Activity at Stalled Forks

To identify potential nucleases and helicases required for processing replication forks after 2 hours exposure to HU, we used siRNAs to knock down enzymes known to act on collapsed forks plus those identified at unperturbed and stalled replication forks through iPOND analysis [27]. Knockdown of EXO1, BLM, and CtIP reduced phospho-CHK1 levels in response to HU, whereas MRE11 knockdown did not (Figure 3*A* and Supplementary Figure 4*A*).

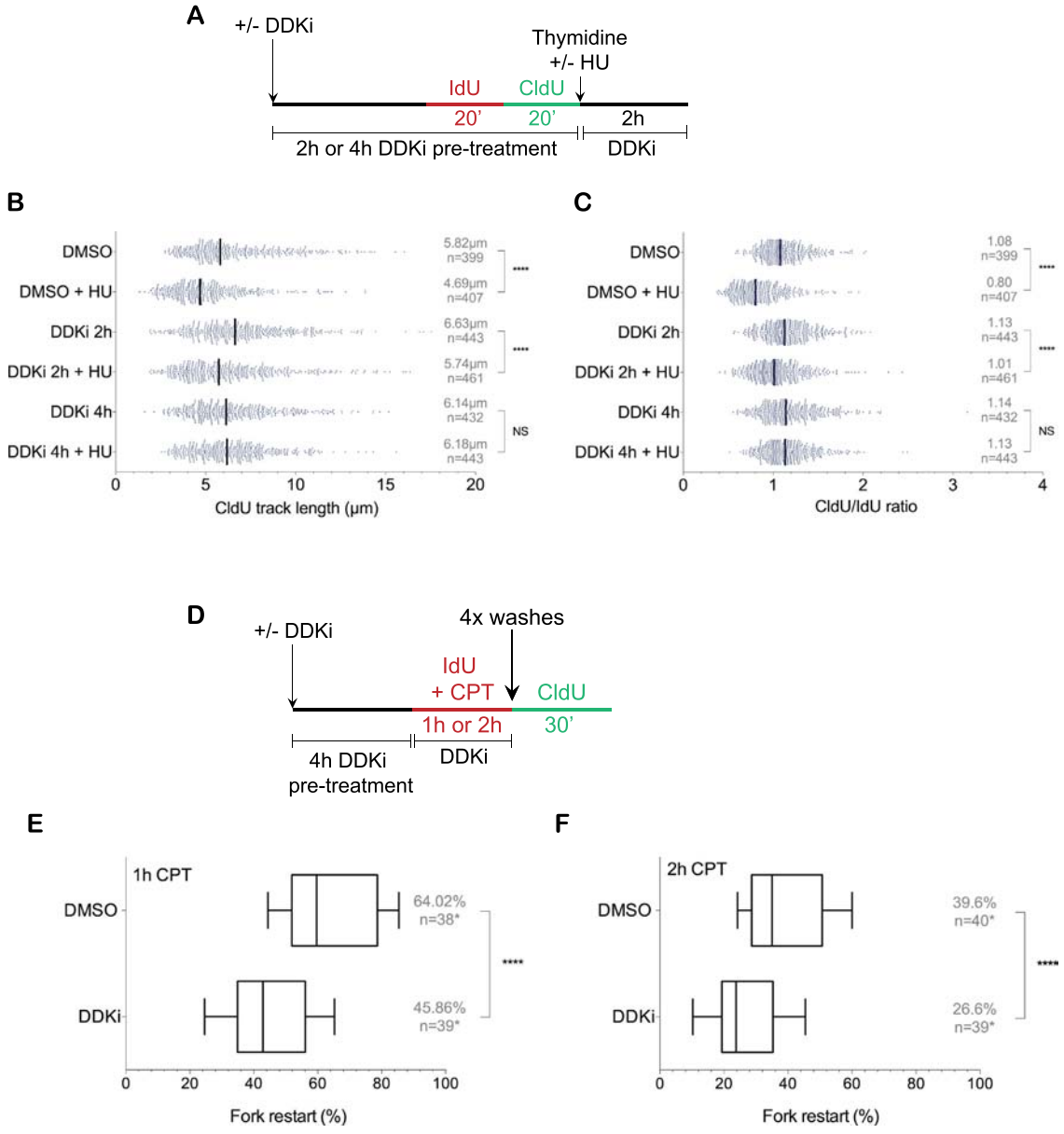

Figure 2. DDK has a primary role in processing and restarting stalled replication forks. (A) HCC1954 cells were pretreated with DMSO or DDKi for 2 or 4 hours, labeled consecutively with IdU and CldU (20 minutes each), subjected to a thymidine chase with or without HU for 2 hours (still in the presence of DDKi (shown) or DMSO), and then harvested for DNA fiber assay. (B, C) Nascent strand resection was measured as the length of CldU tracks (B) or as a ratio of CldU to IdU incorporation (C). (D) HCC1954 cells were pretreated with or without DDKi for 4 hours, exposed to camptothecin (CPT) for 1 or 2 hours in the presence of IdU, washed four times with PBS, and exposed to CldU for a further 30 minutes. Replication fork restart was measured by counting DNA fibers with contiguous IdU and CldU tracks after exposure to 1 hour (E) or 2 hours (F) of CPT. n = xx* in restart assay indicates the number of images counted per sample. Twenty-five to 30 fibers were counted per image.

Knockdown of these enzymes did not significantly affect cell cycle profiles (Supplementary Figure 4*B*). EXO1 knockdown showed the strongest effect on CHK1 phosphorylation, and this was confirmed with two alternate siRNAs against EXO1 (Supplementary Figure 4*C*). We did not observe a reduction in RPA2-S4/S8 phosphorylation upon knockdown of any of the potential resection enzymes. It has been suggested that the initial resection at stalled forks is independent of regression of nascent DNA at stalled forks, which could be the signal for RPA2-S4/S8 phosphorylation [28]. EXO1 knockdown might reduce the extent of nascent DNA degradation (therefore, ssDNA formation and CHK1 phosphorylation) while still allowing fork reversal. Knockdown of the fork regression helicase FBH1 resulted in a decrease in RPA2-S4/S8 phosphorylation after a short HU treatment but had no effect on ATR-CHK1 signaling [28]. Since DDK inhibition results in significant reduction in both CHK1 and RPA2 phosphorylation, this further argues for an upstream role for DDK in replication checkpoint activation.

EXO1 exists in a complex with EEPD1, BLM, and RPA, and knockdown of individual proteins destabilizes other proteins in the complex [29]. Interestingly, EXO1 and BLM are significantly less abundant following exposure to DDKi with or without exposure to DNA damaging agents (Figure 3*B*, **bottom panels**). Moreover,

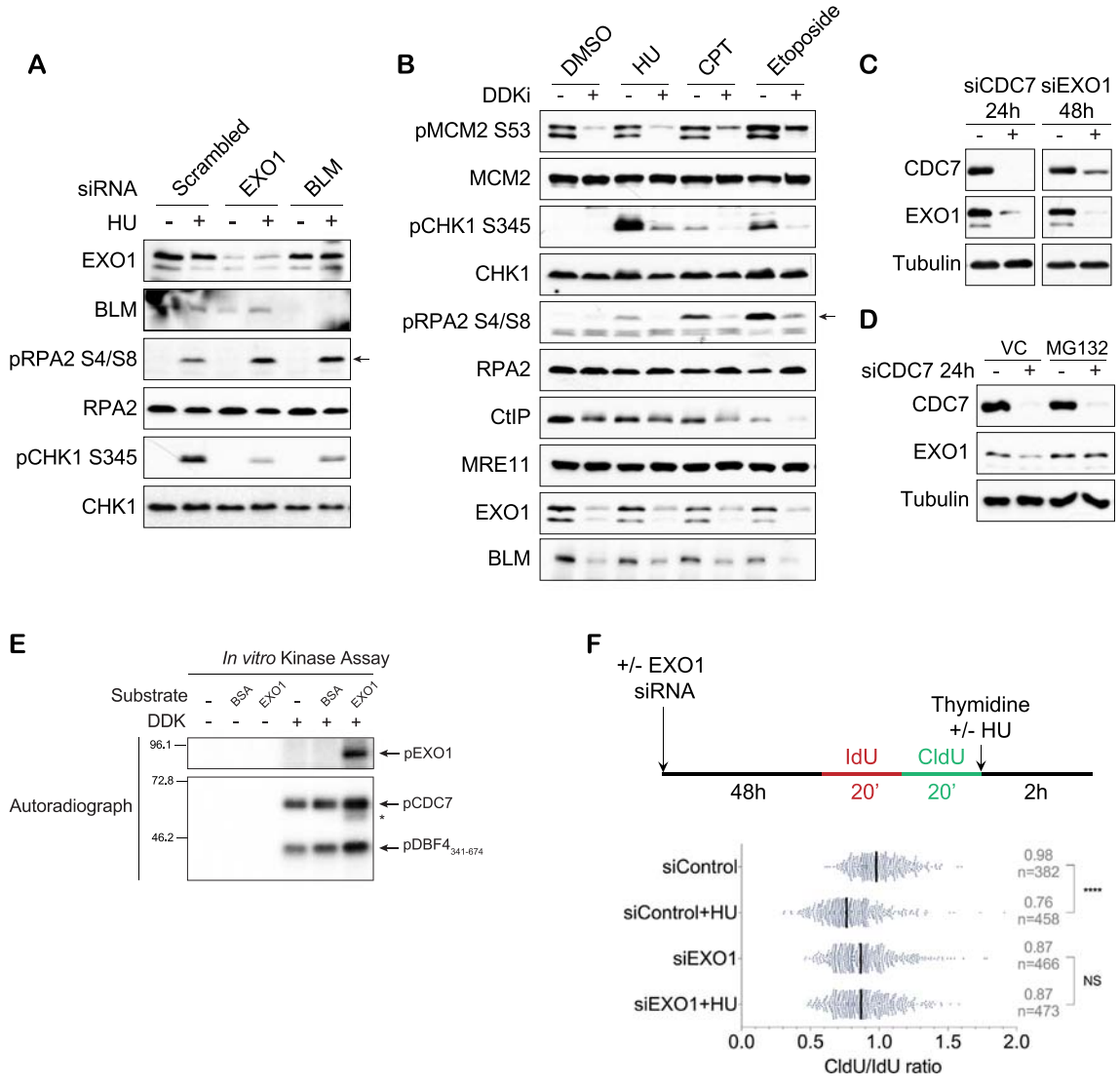

Figure 3. DDK could promote fork resection by directly regulating the activity of nucleases. (A) HCC1954 cells were transfected with indicated siRNAs and 48 hours later treated with or without HU for 2 hours. (B) HCC1954 cells were pretreated with DMSO (−) or DDKi (+) for 4 hours followed by incubation with DMSO, HU, CPT, or etoposide for a further 2 hours. (C) HCC1954 cells were transfected with indicated siRNA for 24 or 48 hours. (D) HCC1954 cells were transfected with CDC7 siRNA and 24 hours later treated with a vehicle control (VC) or MG132 for 3 hours. All samples were analyzed by immunoblot analysis. (E) *In vitro* kinase assay was performed with ~115 ng of purified full length EXO1 and 20 ng of DDK. The asterisk indicates a prominent breakdown product of EXO1. (F) MCF-7 cells were transfected with control or EXO1 siRNA and 48 hours later subjected to DNA fiber assay as in 2A (CldU/IdU ratio).

specifically knocking down either CDC7 or EXO1 significantly reduced expression of the other protein (Figure 3*C*, Supplementary Figure 4*C*). Destabilization of EXO1 could be rescued by treatment with the proteasome inhibitor MG-132, indicating that EXO1 is actively degraded posttranscriptionally in the absence of DDK activity (Figure 3*D*). Overexpression of EXO1, however, was not sufficient to prevent the reduction in CHK1 phosphorylation seen upon DDKi treatment (Supplementary Figure 4*D*). The stability of CtIP was only slightly reduced upon DDK inhibition, and the levels of MRE11 were unchanged (Figure 3*B*). The reduction in HU-induced CHK1 phosphorylation upon CDC7 knockdown was more severe compared to EXO1 knockdown, and co-depletion of both CDC7 and EXO1 did not exacerbate the reduction in CHK1 phosphorylation (Supplementary Figure 4*E*). This suggests that both proteins might act in the same pathway with CDC7 being an upstream regulator with multiple targets. Using purified DDK and EXO1 proteins from bacteria, we found that EXO1 was phosphorylated by DDK *in vitro* (Figure 3*E* and Supplementary Figure 4*F*). EXO1 was not phosphorylated to the same extent as the DDK autophosphorylated bands, so the contrast was increased on the top panel of Figure 3*E*. This indicates that EXO1 is a primary DDK substrate. Since DDK phosphorylation sites are often first primed by Cdk or other kinases in cells at immediately adjacent serines or threonines, EXO1 purified from human cells rather than bacteria might be phosphorylated more extensively by DDK. For instance, Mcm4 is a critical DDK replication target in yeast but can be a relatively poor *in vitro* DDK target depending on how it is purified [30–32]. Further studies are needed to identify the exact DDK-phosphorylation sites on EXO1 and their functional significance *in vivo*. However, our data show that DDK is required for EXO1 stability, perhaps through EXO1

phosphorylation, and suggest an important role for the EXO1-BLM complex in fork resection immediately after fork stalling.

To directly assess the role of EXO1 in regulating nascent strand length when forks stall, we performed DNA fiber analysis in MCF-7 cells transfected with control or EXO1 siRNAs and measured nascent tract lengths after exposure to HU. While control siRNA cells showed the expected reduction in CldU/IdU ratio upon HU exposure, EXO1-depleted cells did not show a similar reduction, indicating that nascent strand resection is reduced upon EXO1 knockdown (Figure 3*F*, Supplementary Figure 4*G*). The cause of reduced basal CldU/IdU ratio in EXO1-depleted cells (Figure 3*F*, 0.87 in siEXO1 vs 0.98 in siControl) is not known. In a separate DNA fiber assay performed in the absence of thymidine chase, nascent DNA tracks were again unaffected by HU in EXO1-depleted cells (Supplementary Figure 4*H*), further

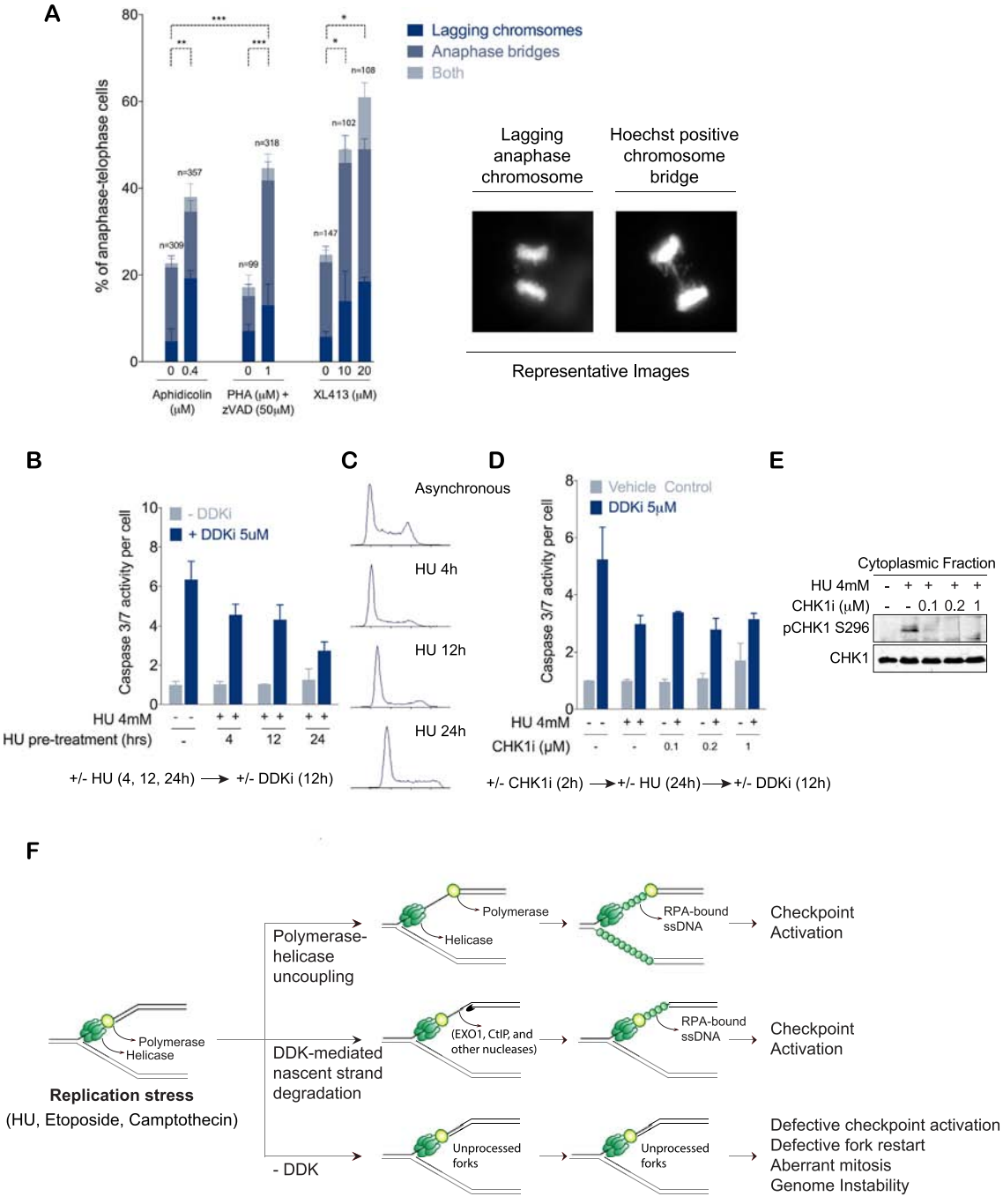

Figure 4. DDK inhibition induces mitotic abnormalities. (A) HCC1954 cells were treated with the indicated drugs for 24 hours and analyzed for mitotic abnormalities. Representative images are shown on the right and quantitated on the left. (B, C) HCC1954 cells were pretreated with HU for the indicated times, analyzed by flow cytometry (C), or incubated with DDKi or DMSO for an additional 12 hours, and assayed for Caspase3/7 activity (B). (D, E) HCC1954 cells were pretreated with varying concentrations of CHK1i for 2 hours, exposed to HU for 24 hours, and then harvested for Western blot (E) or treated with DDKi (dark bars) or DMSO (light bars) for an additional 12 hours prior to assaying for Caspase3/7 activity. (F) Model for role of DDK at stalled replication fork and events downstream of DDK inhibition. We propose DDK-mediated nucleolytic resection of newly synthesized DNA as a mechanism for generation of ssDNA at stalled replication forks.

implicating this nuclease in the nascent strand degradation following HU exposure. Exo1 deletion in fission yeast was recently shown to prevent ssDNA and RPA accumulation at arrested replication forks [33], and EXO1 knockdown in HEK-293 cells significantly reduced ssDNA formation after 2 hours of HU treatment [34], consistent with our finding that EXO1 promotes resection after fork stalling in mammalian cells. We suggest that DDK recruitment to stalled forks facilitates limited nucleolytic removal of nascent DNA involving EXO1, which in turn generates ssDNA-RPA complexes and activates replication checkpoint signaling.

Low-Dose DDKi Causes Aberrant Mitotic Structures

While untransformed human cells prevent S-phase progression upon DDK inhibition by inducing a G1/S-checkpoint [17], tumor cells proceed through an aberrant S-phase and undergo apoptosis, but the exact mechanism that triggers apoptosis remains unknown [17,18]. Inhibiting DDK during S-phase will reduce the number of overall replication forks and inhibit restart of stalled forks (shown here), leading to incomplete DNA replication and a G2/M arrest. However, DDKi-treated cells are also significantly defective in checkpoint activation and would have difficulty restraining mitosis. Our findings therefore prompted us to examine mitotic progression in HCC1954 cells using a low dose of DDKi that will allow S-phase progression. Strikingly, we found numerous aberrant mitotic figures in the DDKi-treated cells similar to cells treated with a low dose (0.4 μM) of aphidicolin, which is known to slow DNA polymerization and induce mitotic abnormalities [35] (Figure 4*A*). The defects in mitosis observed after 24-hour treatment with 1 μM DDKi (PHA) were not a by-product of apoptosis as the same effect was seen both with and without co-treatment with the pan-caspase inhibitor zVAD. To confirm that this effect is DDK-specific, we also tested the more selective biochemical DDK inhibitor XL413 [36]. In HCC1954 cells and many other cell lines, XL413 is a poor *in vivo* inhibitor of DDK activity and has little effect on cell growth even at high inhibitor concentrations [12]. We therefore used relatively high 10-μM and 20-μM concentrations of XL413 to moderately inhibit DDK in HCC1954 cells but not induce apoptosis. We found that XL413 treatment also significantly increased the number of mitotic abnormalities in a dose-dependent manner, confirming this to be a DDK-specific phenotype (Figure 4*A*). Although the increase in lagging chromosomes was similar in aphidicolin and DDKi-treated cells, DDKi treatment resulted in higher number of anaphase bridges compared to aphidicolin-treated cells. Anaphase bridges are thought to arise from chromosomes that have long stretches of incompletely replicated DNA, fused telomeres, or chromatid cohesion defects [37]. Our data suggest that low-level DDKi-treated cells undergo mitosis in presence of underreplicated DNA. Correspondingly, cell cycle arrest by HU pretreatment rescued cell death induced by DDKi, and the extent of rescue was positively correlated with increasing time in HU, with 24 hours of HU pretreatment showing the strongest rescue (Figure 4*B*, *C*). Inhibition of CHK1 activation using a specific CHK1 inhibitor (LY2603618) did not abrogate the rescue seen upon HU pretreatment (Figure 4*D*, *E*). Therefore, preventing S-phase or fork progression protects cells against apoptosis upon DDK inhibition, but active CHK1 is not sufficient for this protection.

Fission yeast cells with hypomorphic DDK mutations also exhibited defective mitosis and DNA fragmentation [5,6]. Importantly, these mutations are synthetically lethal with mutation in the cohesin protein *rad21* [5,6]. These findings have led to the suggestion that DDK has a role in maintaining sister chromatid cohesion following DNA replication. The lack of checkpoint-induced cell cycle arrest, inability to restart naturally stalled forks, and compromised sister chromatid cohesion might explain the severe mitotic abnormalities seen in an asynchronous population of HCC1954 cells with reduced DDK activity.

Conclusions

In summary, we propose that ssDNA generated upon fork stalling is a result of nascent strand degradation that requires DDK (Figure 4*F*). DDK is therefore required for the initiation of replication-checkpoint activation, and we also show for the recovery of stalled forks. An active replication-checkpoint would then attenuate nucleolytic activity at stalled forks to prevent excessive degradation of DNA by described mechanisms [33,38,39]. Budding yeast cells lacking the checkpoint kinase Rad53, which inhibits DDK, exhibited extremely long tracks of ssDNA in presence of replication stress, which were abrogated upon deletion of Exo1 [26], again consistent with our model. Our analysis shows that human EXO1 is phosphorylated by DDK and plays a critical role in nascent strand degradation following exposure to HU, suggesting that DDK regulates EXO1 stability and/or activity. The role of DDK in fork recovery would especially be important within origin poor regions of the genome where forks are known to stall. Since stalled forks cannot activate a robust checkpoint response in the absence of DDK, cells progress into M-phase with underreplicated DNA. Aberrant anaphase progression would result in chromosomal breakage and genomic instability and might be the primary cause of cell death in DDKi-treated cancer cells (Figure 4*F*).

Author Contributions

N. K. S., F. C., and Y.-L. L. performed all the experiments. J. P. M., P. P., and M. W. designed the experiments; N. K. S. and M. W. wrote the manuscript.

Acknowledgements

We thank Bruce Stillman (Cold Spring Harbor) for the RPA antibodies, Peter Cherepanov (Francis Crick Institute) for DDK constructs, and Titia de Lange (Rockefeller University) for reagents and guidance. This work was supported by the NIH National Cancer Institute (grant R01CA197398 to J.P.M.); the Van Andel Institute (M.W., N.K.S., and J.P.M.); and the Michigan State University (N.K.S.). Work in the Pasero laboratory is supported by the Institut National du Cancer (INCa) and the Ligue contre le Cancer (équipe labellisée).

Conflict of Interests

The authors declare that they have no conflict of interest.

Appendix A. Supplementary Data

Supplementary data to this article can be found online at https://doi.org/10.1016/j.neo.2018.08.001.

References

[1] Sasi NK and Weinreich M (2016). DNA replication checkpoint signaling. In: Kaplan LD, editor. The initiation of dna replication in eukaryotes. Cham: Springer International Publishing; 2016. p. 479–502.

[2] Weinreich M and Stillman B (1999). Cdc7p-Dbf4p kinase binds to chromatin during S phase and is regulated by both the APC and the RAD53 checkpoint pathway. *EMBO J* **18**(19), 5334–5346. https://doi.org/10.1093/emboj/18.19.5334 [Epub 1999/10/03, PubMed PMID: 10508166; PubMed Central PMCID: PMC1171603].

[3] Zegerman P and Diffley JF (2010). Checkpoint-dependent inhibition of DNA replication initiation by Sld3 and Dbf4 phosphorylation. *Nature* **467**(7314), 474–478. https://doi.org/10.1038/nature09373.

[4] Ogi H, Wang CZ, Nakai W, Kawasaki Y, and Masumoto H (2008). The role of the Saccharomyces cerevisiae Cdc7-Dbf4 complex in the replication checkpoint. *Gene* **414**(1–2), 32–40. https://doi.org/10.1016/j.gene.2008.02.010 [PubMed PMID: 18372119].

[5] Snaith HA, Brown GW, and Forsburg SL (2000). Schizosaccharomyces pombe Hsk1p is a potential cds1p target required for genome integrity. *Mol Cell Biol* **20** (21), 7922–7932 [PubMed PMID: 11027263; PubMed Central PMCID: PMCPMC86403].

[6] Takeda T, Ogino K, Tatebayashi K, Ikeda H, Arai K, and Masai H (2001). Regulation of initiation of S phase, replication checkpoint signaling, and maintenance of mitotic chromosome structures during S phase by Hsk1 kinase in the fission yeast. *Mol Biol Cell* **12**(5), 1257–1274.

[7] Dierov J, Dierova R, and Carroll M (2004). BCR/ABL translocates to the nucleus and disrupts an ATR-dependent intra-S phase checkpoint. *Cancer Cell* **5** (3), 275–285.

[8] Tenca P, Brotherton D, Montagnoli A, Rainoldi S, Albanese C, and Santocanale C (2007). Cdc7 is an active kinase in human cancer cells undergoing replication stress. *J Biol Chem* **282**(1), 208–215. https://doi.org/10.1074/jbc.M604457200.

[9] Yamada M, Watanabe K, Mistrik M, Vesela E, Protivankova I, Mailand N, Lee M, Masai H, Lukas J, and Bartek J (2013). ATR-Chk1-APC/CCdh1-dependent stabilization of Cdc7-ASK (Dbf4) kinase is required for DNA lesion bypass under replication stress. *Genes Dev* **27**(22), 2459–2472. https://doi.org/10.1101/gad.224568.113 [Epub 2013/11/19, PubMed PMID: 24240236; PubMed Central PMCID: PMC3841735].

[10] Kim JM, Kakusho N, Yamada M, Kanoh Y, Takemoto N, and Masai H (2008). Cdc7 kinase mediates Claspin phosphorylation in DNA replication checkpoint. *Oncogene* **27**(24), 3475–3482. https://doi.org/10.1038/sj.onc.1210994 [PubMed PMID: 18084324].

[11] Rainey MD, Harhen B, Wang GN, Murphy PV, and Santocanale C (2013). Cdc7-dependent and -independent phosphorylation of Claspin in the induction of the DNA replication checkpoint. *Cell Cycle* **12**(10), 1560–1568. https://doi.org/10.4161/cc.24675 [PubMed PMID: 23598722; PubMed Central PMCID: PMCPMC3680535].

[12] Sasi NK, Tiwari K, Soon FF, Bonte D, Wang T, Melcher K, Xu HE, and Weinreich M (2014). The potent Cdc7-Dbf4 (DDK) kinase inhibitor XL413 has limited activity in many cancer cell lines and discovery of potential new DDK inhibitor scaffolds. *PLoS One* **9**(11)e113300. https://doi.org/10.1371/journal.pone.0113300 [PubMed PMID: 25412417; PubMed Central PMCID: PMCPMC4239038].

[13] Mendez J and Stillman B (2000). Chromatin association of human origin recognition complex, cdc6, and minichromosome maintenance proteins during the cell cycle: assembly of prereplication complexes in late mitosis. *Mol Cell Biol* **20**(22), 8602–8612 [PubMed PMID: 11046155; PubMed Central PMCID: PMCPMC102165].

[14] Jackson DA and Pombo A (1998). Replicon clusters are stable units of chromosome structure: evidence that nuclear organization contributes to the efficient activation and propagation of S phase in human cells. *J Cell Biol* **140**(6), 1285–1295 [PubMed PMID: 9508763; PubMed Central PMCID: PMCPMC2132671].

[15] Breslin C, Clements PM, El-Khamisy SF, Petermann E, Iles N, and Caldecott KW (2006). Measurement of chromosomal DNA single-strand breaks and replication fork progression rates. *Methods Enzymol* **409**, 410–425. https://doi.org/10.1016/S0076-6879(05)09024-5 [PubMed PMID: 16793415].

[16] El-Shemerly M, Janscak P, Hess D, Jiricny J, and Ferrari S (2005). Degradation of human exonuclease 1b upon DNA synthesis inhibition. *Cancer Res* **65**(9), 3604–3609. https://doi.org/10.1158/0008-5472.CAN-04-4069 [PubMed PMID: 15867354].

[17] Montagnoli A, Tenca P, Sola F, Carpani D, Brotherton D, Albanese C, and Santocanale C (2004). Cdc7 inhibition reveals a p53-dependent replication checkpoint that is defective in cancer cells. *Cancer Res* **64**(19), 7110–7116. https://doi.org/10.1158/0008-5472.CAN-04-1547 [Epub 2004/10/07, PubMed PMID: 15466207].

[18] Montagnoli A, Valsasina B, Croci V, Menichincheri M, Rainoldi S, Marchesi V, Tibolla M, Tenca P, Brotherton D, and Albanese C, et al (2008). A Cdc7 kinase inhibitor restricts initiation of DNA replication and has antitumor activity. *Nat Chem Biol* **4**(6), 357–365. https://doi.org/10.1038/nchembio.90 [Epub 2008/05/13, PubMed PMID: 18469809].

[19] Vassin VM, Anantha RW, Sokolova E, Kanner S, and Borowiec JA (2009). Human RPA phosphorylation by ATR stimulates DNA synthesis and prevents ssDNA accumulation during DNA-replication stress. *J Cell Sci* **122**(Pt 22), 4070–4080. https://doi.org/10.1242/jcs.053702 [PubMed PMID: 19843584; PubMed Central PMCID: PMCPMC2776501].

[20] Toledo LI, Altmeyer M, Rask M-BB, Lukas C, Larsen DH, Povlsen LK, Bekker-Jensen S, Mailand N, Bartek J, and Lukas J (2013). ATR prohibits replication catastrophe by preventing global exhaustion of RPA. *Cell* **155**(5), 1088–1103. https://doi.org/10.1016/j.cell.2013.10.043.

[21] Gabrielse C, Miller CT, McConnell KH, DeWard A, Fox CA, and Weinreich M (2006). A Dbf4p BRCA1 C-terminal-like domain required for the response to replication fork arrest in budding yeast. *Genetics* **173**(2), 541–555. https://doi.org/10.1534/genetics.106.057521.

[22] Byun TS, Pacek M, Yee M-cC, Walter JC, and Cimprich KA (2005). Functional uncoupling of MCM helicase and DNA polymerase activities activates the ATR-dependent checkpoint. *Genes Dev* **19**(9), 1040–1052. https://doi.org/10.1101/gad.1301205.

[23] Kim S, Dallmann HG, McHenry CS, and Marians KJ (1996). Coupling of a replicative polymerase and helicase: a tau-DnaB interaction mediates rapid replication fork movement. *Cell* **84**(4), 643–650 [PubMed PMID: 8598050].

[24] Stano NM, Jeong YJ, Donmez I, Tummalapalli P, Levin MK, and Patel SS (2005). DNA synthesis provides the driving force to accelerate DNA unwinding by a helicase. *Nature* **435**(7040), 370–373. https://doi.org/10.1038/nature03615 [PubMed PMID: 15902262; PubMed Central PMCID: PMCPMC1563444].

[25] Langston LD, Zhang D, Yurieva O, Georgescu RE, Finkelstein J, Yao NY, Indiani C, and O'Donnell ME (2014). CMG helicase and DNA polymerase epsilon form a functional 15-subunit holoenzyme for eukaryotic leading-strand DNA replication. *Proc Natl Acad Sci U S A* **111**(43), 15390–15395. https://doi.org/10.1073/pnas.1418334111 [PubMed PMID: 25313033; PubMed Central PMCID: PMCPMC4217400].

[26] Sogo JM, Lopes M, and Foiani M (2002). Fork reversal and ssDNA accumulation at stalled replication forks owing to checkpoint defects. *Science* **297**(5581), 599–602. https://doi.org/10.1126/science.1074023.

[27] Sirbu BM, McDonald WH, Dungrawala H, Badu-Nkansah A, Kavanaugh GM, Chen Y, Tabb DL, and Cortez D (2013). Identification of proteins at active, stalled, and collapsed replication forks using isolation of proteins on nascent DNA (iPOND) coupled with mass spectrometry. *J Biol Chem* **288**(44), 31458–31467. https://doi.org/10.1074/jbc.M113.511337 [PubMed PMID: 24047897; PubMed Central PMCID: PMCPMC3814742].

[28] Fugger K, Mistrik M, Neelsen KJ, Yao Q, Zellweger R, Kousholt AN, Haahr P, Chu WK, Bartek J, and Lopes M, et al (2015). FBH1 catalyzes regression of stalled replication forks. *Cell Rep* . https://doi.org/10.1016/j.celrep.2015.02.028 [PubMed PMID: 25772361].

[29] Wu Y, Lee SH, Williamson EA, Reinert BL, Cho JH, Xia F, Jaiswal AS, Srinivasan G, Patel B, and Brantley A, et al (2015). EEPD1 rescues stressed replication forks and maintains genome stability by promoting end resection and homologous recombination repair. *PLoS Genet* **11**(12)e1005675. https://doi.org/10.1371/journal.pgen.1005675 [PubMed PMID: 26684013; PubMed Central PMCID: PMCPMC4684289].

[30] Kihara M, Nakai W, Asano S, Suzuki A, Kitada K, Kawasaki Y, Johnston LH, and Sugino A (2000). Characterization of the yeast Cdc7p/Dbf4p complex purified from insect cells. Its protein kinase activity is regulated by Rad53p. *J Biol Chem* **275** (45), 35051–35062. https://doi.org/10.1074/jbc.M003491200 [PubMed PMID: 10964916].

[31] Sheu Y-JJ and Stillman B (2010). The Dbf4-Cdc7 kinase promotes S phase by alleviating an inhibitory activity in Mcm4. *Nature* **463**(7277), 113–117. https://doi.org/10.1038/nature08647.

[32] Randell JC, Fan A, Chan C, Francis LI, Heller RC, Galani K, and Bell SP (2010). Mec1 is one of multiple kinases that prime the Mcm2-7 helicase for phosphorylation by Cdc7. *Mol Cell* **40**(3), 353–363. https://doi.org/10.1016/j.molcel.2010.10.017.

[33] Ait Saada A, Teixeira-Silva A, Iraqui I, Costes A, Hardy J, Paoletti G, Freon K, and Lambert SAE (2017). Unprotected replication forks are converted into mitotic sister chromatid bridges. *Mol Cell* **66**(3), 398–410.e4. https://doi.org/10.1016/j.molcel.2017.04.002 [PubMed PMID: 28475874].

[34] Kim HS, Nickoloff JA, Wu Y, Williamson EA, Sidhu GS, Reinert BL, Jaiswal AS, Srinivasan G, Patel B, and Kong K, et al (2017). Endonuclease EEPD1 is a

gatekeeper for repair of stressed replication forks. *J Biol Chem* **292**(7), 2795–2804. https://doi.org/10.1074/jbc.M116.758235 [PubMed PMID: 28049724; PubMed Central PMCID: PMCPMC5314175].

[35] Le Beau MM, Rassool FV, Neilly ME, Espinosa 3rd R, Glover TW, Smith DI, and McKeithan TW (1998). Replication of a common fragile site, FRA3B, occurs late in S phase and is delayed further upon induction: implications for the mechanism of fragile site induction. *Hum Mol Genet* **7**(4), 755–761 [PubMed PMID: 9499431].

[36] Koltun ES, Tsuhako AL, Brown DS, Aay N, Arcalas A, Chan V, Du H, Engst S, Ferguson K, and Franzini M, et al (2012). Discovery of XL413, a potent and selective CDC7 inhibitor. *Bioorg Med Chem Lett* **22**(11), 3727–3731. https://doi.org/10.1016/j.bmcl.2012.04.024 [Epub 2012/05/09, PubMed PMID: 22560567].

[37] Maciejowski J and de Lange T (2017). Telomeres in cancer: tumour suppression and genome instability. *Nat Rev Mol Cell Biol* **18**(3), 175–186. https://doi.org/10.1038/nrm.2016.171 [PubMed PMID: 28096526].

[38] El-Shemerly M, Hess D, Pyakurel AK, Moselhy S, and Ferrari S (2008). ATR-dependent pathways control hEXO1 stability in response to stalled forks. *Nucleic Acids Res* **36**(2), 511–519. https://doi.org/10.1093/nar/gkm1052 [PubMed PMID: 18048416; PubMed Central PMCID: PMCPMC2241874].

[39] Schlacher K, Christ N, Siaud N, Egashira A, Wu H, and Jasin M (2011). Double-strand break repair-independent role for BRCA2 in blocking stalled replication fork degradation by MRE11. *Cell* **145**(4), 529–542. https://doi.org/10.1016/j.cell.2011.03.041 [PubMed PMID: 21565612; PubMed Central PMCID: PMCPMC3261725].